The Mystery of the Subsurface Fluorescence Layer and Green Sulphur Bacteria in Byfjorden

Tibaud Cardis, Aryan Kaura, Hedda Matteoni and Adéla Zvěřinová

Supervisor: Erik Selander

University of Gothenburg

MAR440

Abstract

Byfjorden is a sill fjord with anoxic bottom water below the sill depth. Previous course cruises have consistently observed an unexplained strong fluorescent layer in the transition zone between oxic and anoxic water, at approximately 20 m depth. Here we show new insights into probable causes behind this subsurface fluorescence layer. The phenomenon is usually connected to phytoplankton blooms with a chlorophyll *a* maxima. However, High-Performance Liquid Chromatography showed only trace amounts of chlorophyll *a* in the subsurface fluorescence layer. Instead, absorption spectra of the pigments from the subsurface fluorescence layer revealed a strong resemblance to that of bacteriochlorophyll *e*. Mass spectrometry also suggests that the pigments consist of closely related derivatives of bacteriochlorophyll *e*. This pigment can be found in green sulphur bacteria which inhabit environments with similar conditions to Byfjorden. These microorganisms perform anoxygenic photosynthesis by utilising reduced sulphur compounds as an electron donor. Our results are the starting point for further research regarding green sulphur bacteria in stratified and anoxic fjords. However, genetic analysis should be carried out to verify the presence of green sulphur bacteria in the fjord.

1. Introduction

The spread of anoxic zones is a global environmental problem (Diaz & Rosenberg 2008). Although hypoxic waters can occur naturally in nutrient rich areas with coastal upwelling (Helly & Levin 2004), anthropogenic influence and eutrophication has led to an increased occurrence of anoxic waters in coastal habitats, fjords, and estuaries (Diaz & Rosenberg 2008, Rabalais et al. 2010). Water masses affected by long term or intense hypoxia face community structure change. Almost all macrofauna is eradicated and the secondary production reduces radically, leading to the trophic energy being shifted to microbes (Diaz & Rosenberg 1995).

As Klausmeier and Litchman (2001) pointed out, the contrasting gradient of resources in stratified waters (i.e. light from above and nutrients from below) essentially leads to the subsurface biomass and in many cases a chlorophyll *a* maximum, which could cause a subsurface fluorescence peak (hereafter fluorescence layer). These can be linked to phytoplankton blooms, which are quite common and have been recorded all over the world's oceans (eg. Nielsen et al. 1990, Legović et al. 1991, Perry et al. 2008, Padmakumar et al. 2018, Baldry et al. 2020). They were reported from stratified eutrophic waters (Legović et al. 1991) or areas with calm conditions and depleted nutrients at the surface (Nielsen et al. 1990, Lips et al. 2010, Baldry et al. 2020). In some cases, the blooms occur below the euphotic layer as well (Kanonen et al. 2003).

Another possible explanation for a fluorescence layer is the presence of bacteria. As Koskinenn et al. (2011) showed, bacterial communities are found all throughout the water column in the Baltic Sea, and their structure is highly affected by physical and hydrochemical conditions. While cyanobacteria live and thrive in oxic conditions, anoxygenic phototrophic bacteria need an anaerobic environment (Imhoff 1992). The one exception is aerobic anoxygenic phototrophic bacteria that need oxygen to grow, but do not produce it. They inhabit a wide variety of eutrophic aquatic environments and utilise bacteriochlorophyll *a* as the main photosynthetic pigment, together with a variety of carotenoids (Yurkov & Beatty 1998). Anaerobic phototrophic bacteria are generally divided into two groups, based on the pigments they contain: purple sulphur bacteria with bacteriochlorophyll *a*, *b* and carotenoids, and green sulphur bacteria with bacteriochlorophyll *c*, *d* and *e* (Imhoff 1992). Since cyanobacteria perform oxygenic photosynthesis they rather use chlorophylls (mainly chlorophyll *a*), carotenoids and phycobilisomes (Saini et al., 2018).

Lastly, biomass and materials tend to accumulate at the pycnocline (Franks 1992, Andersen & Nielsen 2002, Chen et al., 2004). Part of dissolved organic matter in the ocean, the chromophoric dissolved organic matter, can be optically measured and shows fluorescent properties (Röttgers & Koch 2012, Stedmon & Nelson 2015), which could therefore result in a fluorescence spike.

Byfjorden is a 4 km long and 1.2 km wide fjord located on the west coast of Sweden. It reaches a maximum depth of 51 m and is characterised by anoxic basin water and stratification due to weak

vertical mixing (Stigebrandt & Liljebladh 2010). The course MAR440 has revisited Byfjorden for sampling for six years and has continuously reported a marked subsurface fluorescent layer around 20 m depth. Up to this day, no explanation for this fluorescence layer has been put forward. Our goal for this report is to find a probable cause of the fluorescence layer. To identify a possible explanation we carried out detailed pigment analyses and identified and quantified microorganisms from water samples collected in Byfjorden and Havstensfjorden.

2. Method and Materials

2.1 Sample Collection

We visited a total of nine stations along a transect inside Byfjorden and the neighbouring fjord, Havstensfjorden, on the 7th of September 2022 (Figure 1). A CTD-Rosette (model: SeaBird911, rosette sampler: SBE 32, 24 bottles (8 l)) present aboard the R/V Skagerak was used to collect data at all nine stations regarding oxygen, salinity, temperature, fluorescence and turbidity. Stations 1-7 were used to collect water samples using Niskin bottles. Water samples were collected from the fluorescence layer observed at 20-22 m, as well as the surface at 0-7m. Each sample was stored in one 1 litre and one 100 ml bottle. Samples in the 100 ml bottles were fixed with Lugol's iodine solution.

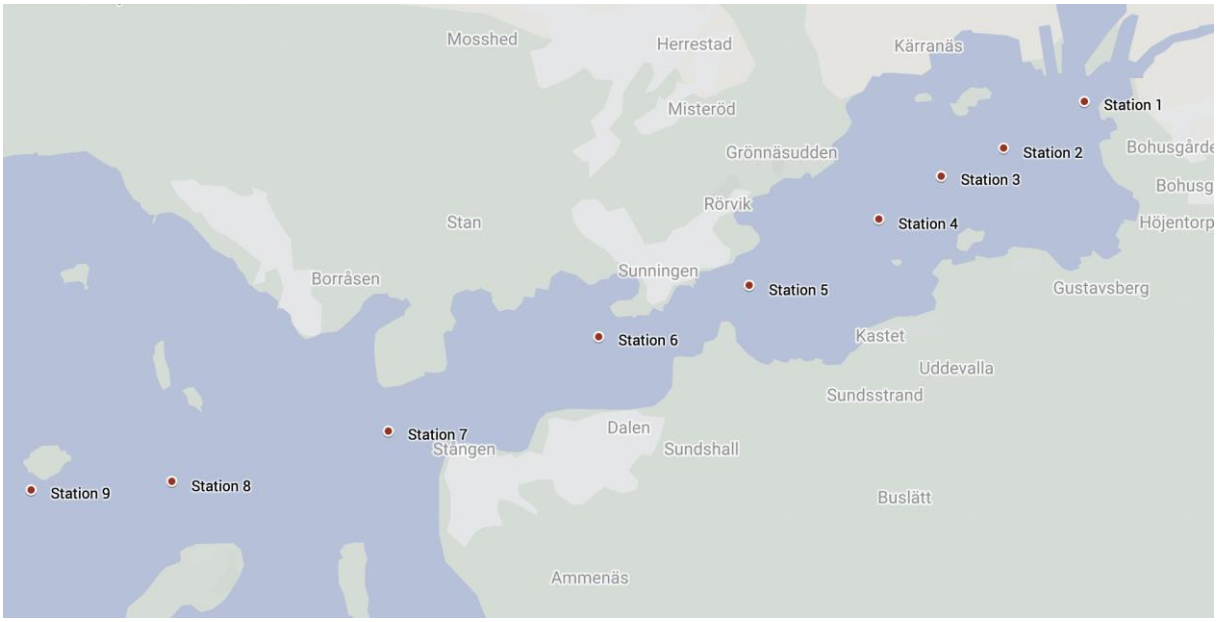

Figure 1. Map of the sample collection site with individual stations marked.

2.2 Solid Phase Extraction and Fluorometric Analysis

We ran 200 ml of untreated water samples through ABN columns (Argonaut Evolute SPE columns ABN) to perform solid phase extraction. The columns were washed with 3 ml of MilliQ water to remove excess salt and eluted 2*1.5 methanol separated by a 30 second soakstep. We transferred 2 ml of each sample into cuvettes and ran them in a fluorometer (Turner Designs, Trilogy), using a chlorophyll *a* module (excitation: 436/10 nm, emission filter wavelengths: 685/10 nm). Cuvettes with 2 ml of methanol were used as a control.

2.3 High-Performance Liquid Chromatography

Three samples from the subsurface fluorescence layer and three samples from the surface were suction filtered (16.66 kP) onto a glass microfiber filter (Whatman, GF/F, diameter = 25 mm, see appendix Table 2 for filtered volumes). The filters were wrapped in aluminium foil and stored in Eppendorf tubes in the freezer. The filters were submerged in 3 ml of extraction buffer (8:2, acetone:methanol; v/v) overnight. Analysis was carried out in a low light environment to prevent pigment degradation. We filtered these samples through 15 mm hydrophilic syringe filters and put 100 µl in vials. The six samples were then placed in an array with a chlorophyll *a* standard, two vials containing the extraction buffer, as well as three vials with methanol that acted as cleansers. We then performed High-Performance Liquid Chromatography (HPLC) on the array (Shimadzu, LC20AD coupled to a SPD-M20A diode array detector). The gradient phase used consisted of three elements; mobile phase A: 85% methanol (aq) and

15% 0.5 M ammonium acetate buffer with a pH of 7.2, mobile phase B: 90% acetonitrile (aq) and mobile phase C: 100% ethyl acetate. The gradient elution went from 100% A to 90% B the first eight minutes of running the sample and then the level of C gradually increased from 35 % to 69% until 25 minutes.

2.4 Mass Spectrometry

We pooled the pigment samples from the fluorescent layer and concentrated them by evaporating the solvent at 40°C under a stream of nitrogen. This concentrated sample was run through the HPLC system, and the peak samples were collected through the outflow pipe 10 seconds after the peaks were identified on the monitor (see appendix for calculation). These samples were then run through the mass spectrometer (Agilent Technologies, 6470 Triple Quad LC/MS), with a direct infusion buffer (35% acetonitrile, 35% methanol and 30% MilliQ water with 0.2 % formic acid; v/v) and a flow rate of 0.2 ml/min to identify and isolate possible fluorescent molecules. The ion source was operated at 260ºC with a gas flow of 6 l/min and a capillary voltage of 3500 V. MS2 scan was used to scan for fragments with mass ranging from 100- 1000 m/z. The fragmentation experiment was carried out in negative mode, at 135 V with a collision energy of 48 V. After the mass spectrometry the samples were diluted with 2

ml of extraction buffer and run through the fluorometer to confirm fluorescence. Blanks were measured using the extraction buffer.

2.5 Microscopy and Taxonomy

Three samples each from the surface and subsurface fluorescent layer were sedimented overnight in Utermöhl chambers with a volume of 50 ml. The samples were degassed prior to sedimentation to prevent the formation of air bubbles. We identified and enumerated the plankton species manually using a light microscope (Zeiss AxioVert A1 with 40x magnification and Zeiss Axiovert 49 CFl with 40x magnification).

2.6 Fluorescent Microscopy

We pipetted two drops of Lugol-fixed sample as well as two drops of untreated water sample onto separate slides, and studied them under a fluorescent microscope(Zeiss Axio Scope A1) set to the mode CFP (excitation: BP 395-440, beam-splitter: FT 460, emission: LP 470). These samples were studied in a dark room with green light.

3. Results

3.1 Hydrography

A distinct fluorescence layer can be observed around 20 m depth within Byfjorden (Figure 3). This fluorescence layer has more than two times higher chlorophyll *a* equivalence concentration than the surface waters.

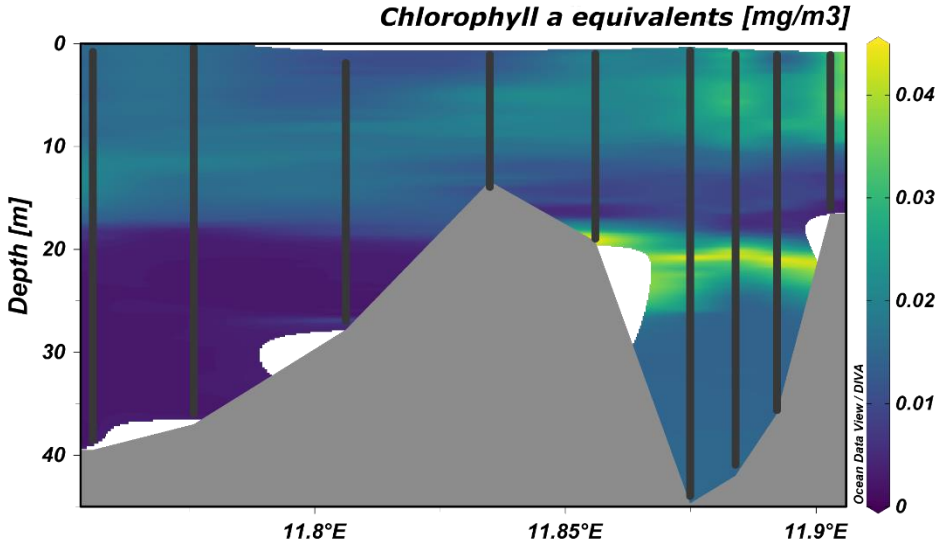

Figure 3. Chlorophyll *a* equivalence concentration (mg/m^3) along the longitudinal transect in the By Fjord. Each line represents a station, going from Station 1 on the right to Station 9 on the left.

The fluorescence level in Havstenssfjorden is the highest in the surface waters, specifically around 7-12 m depth (Figure 4, B and D). In Byfjorden, the equivalent depth is 20-22 m depth (Figure 4, A and C). The depths of the thermocline, halocline and oxycline also differ between the two fjords. In Byfjorden, the thermocline, halocline and oxycline are located at 10-15 m depth (Figure 4, A). However, in Havstensfjorden these are found at larger depths, around 12-20 m (Figure 4, B). In Byfjorden (Figure 4, C) a peak in turbidity can be observed 1-2 m below the subsurface fluorescence peak. This phenomenon is absent in Havstensfjorden (Figure 4, D).

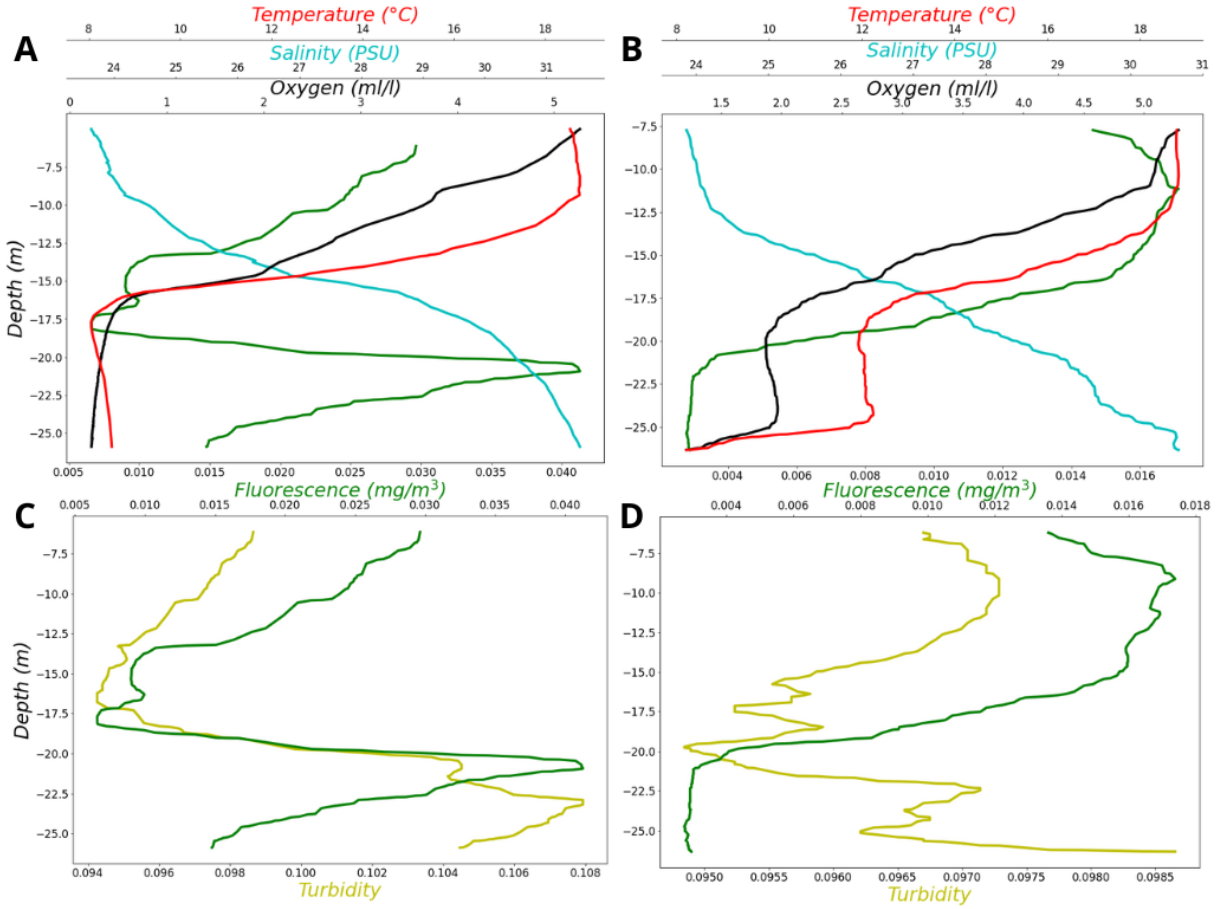

Figure 4. CTD-profiles showing temperature, salinity, oxygen and fluorescence for A: Byfjorden and B: Havstensfjorden. Below are CTD-profiles showing fluorescence and turbidity for C: Byfjorden and D: Havstensfjorden.

3.2 Fluorometric Analysis

The mean chlorophyll *a* equivalents concentration in the fluorescent layer was eight times higher than in the surface samples and was statistically significant ($t_4 = 13.285$, $p = 0.0002$, Figure 5).

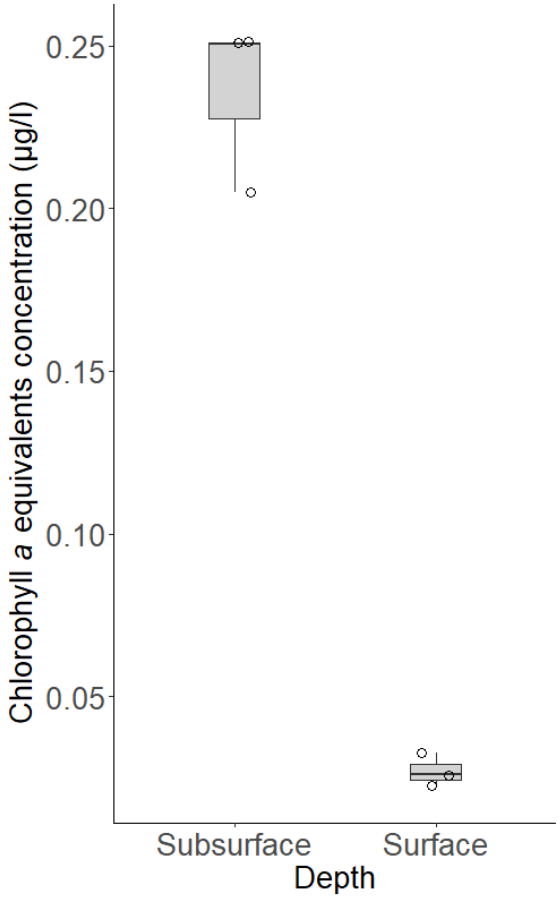

Figure 5. The chlorophyll *a* equivalents concentration (µg/l) at subsurface fluorescence layer and surface samples inside of the By fjord. n = 3. Upper and lower quartiles, median and whiskers indicating range of values outside quartiles are shown. Stations are represented as points.

3.3 High-Performance Liquid Chromatography

The surface sample (Station 3 / 7m) is consistent with the chlorophyll *a* standard with a peak at 21.93 minutes (P3 and P4, Figure 7) and indicates the presence of chlorophyll *a*. This peak was not found in the fluorescence layer sample (Station 3 / 21m). In comparison, the fluorescence layer sample shows only trace amounts of chlorophyll *a* and instead exhibits a unique pigment signature which is represented by two prominent peaks at 15.98 minutes and 16.91 minutes (P1 and P2, Figure 6).

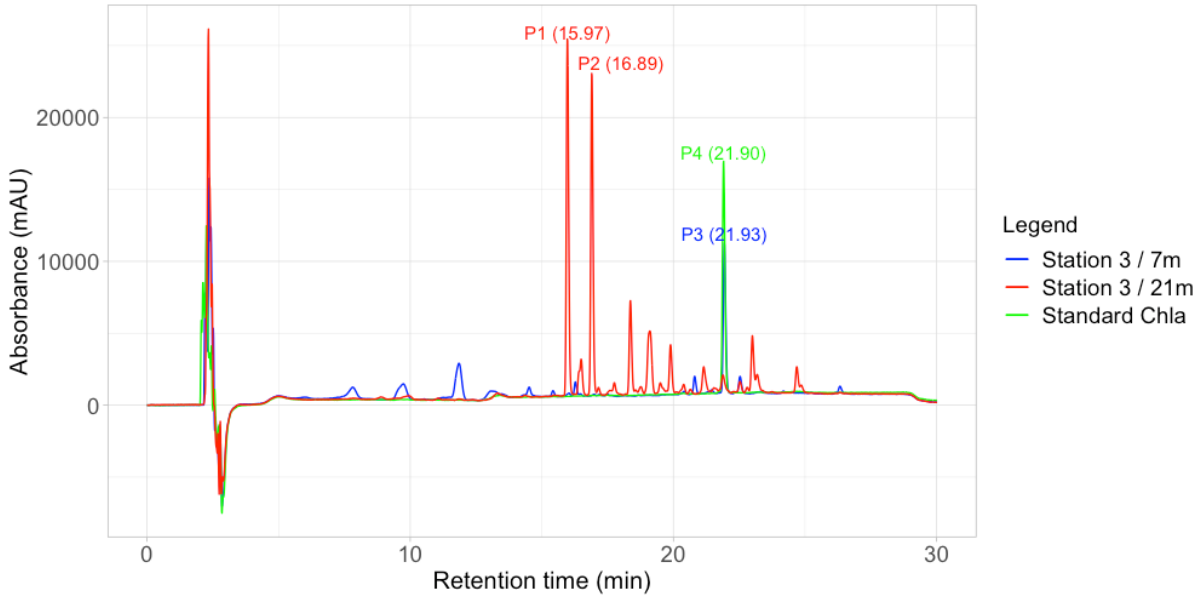

Figure 6. High-performance liquid chromatogram of surface and subsurface samples, together with a chlorophyll *a* standard.

The absorption spectra of the two peaks from the fluorescence layer samples are nearly identical (Station 3 / 21m P1 and Station 3 / 21m P2, Figure 7). The absorption spectrum from the peak at 21.93 from the surface sample (Station 3 / 7m P3, Figure 7) resembles the absorption spectrum of the chlorophyll *a* standard (Chla P4, Figure 7).

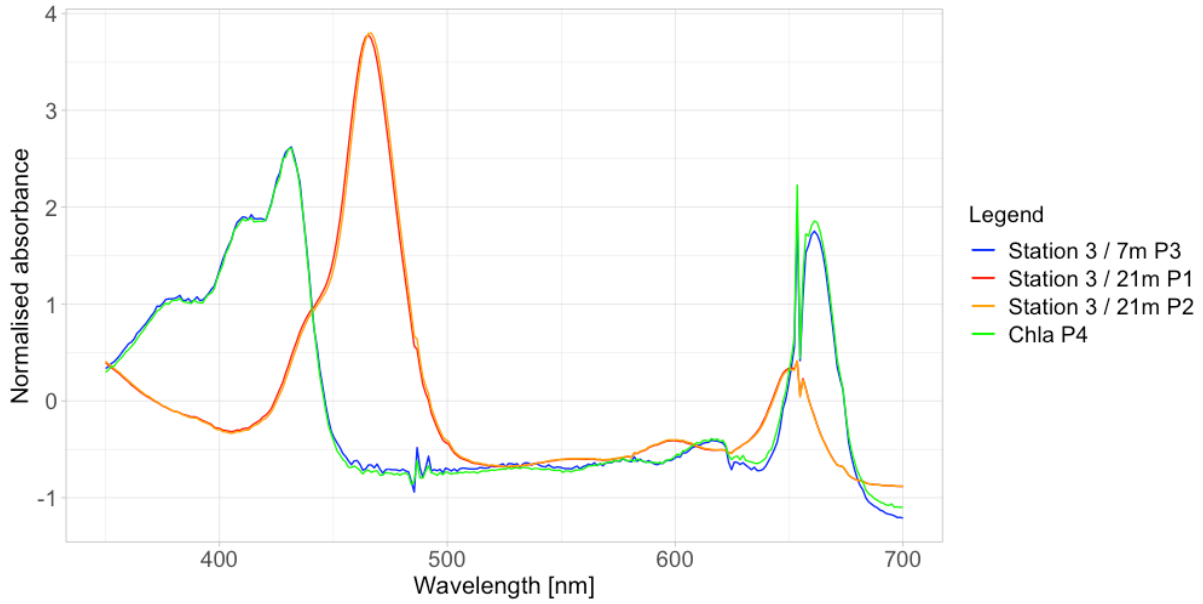

Figure 7. Absorption spectra for surface sample peak (P3), fluorescence layer sample peaks (P1 and P2) and chlorophyll *a* standard (P4).

The absorption spectrum for subsurface samples shows a strong resemblance to that of bacteriochlorophyll *e* (Figure 8).

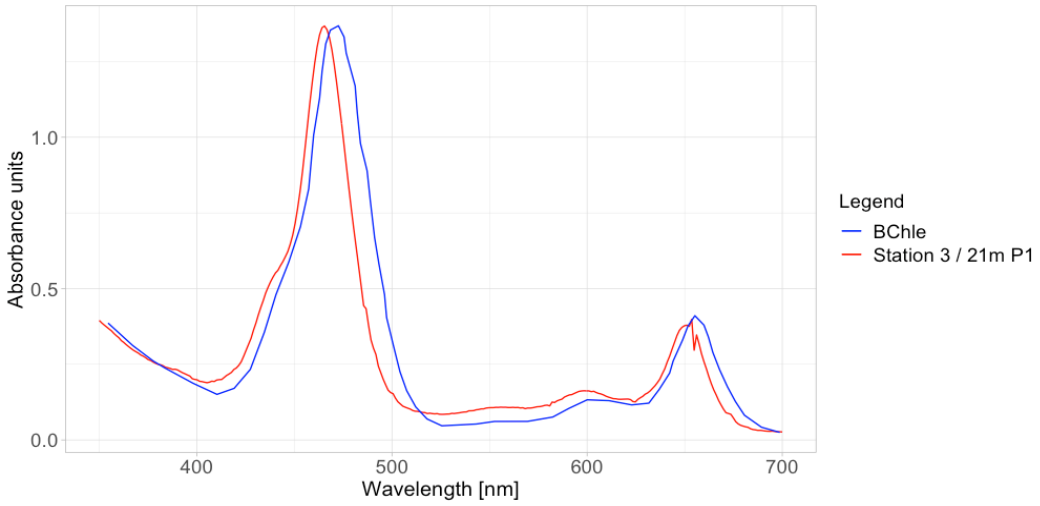

Figure 8. Absorption spectra of Station 3, 21 m (P1, extraction buffer: 8:2 acetone:methanol; v/v) and bacteriochlorophyll *e* (extraction buffer: ethanol) from Borrego *et al.*, 1999.

3.4 Mass Spectrometry

The mass spectrum from the two peaks from the HPLC resulted in five fragments with abundance above 60 for Peak 1 and two fragments with abundance over 60 for Peak 2 (Figure 9). The mother ions can be seen to the right in the graphs, 865.4 m/z (M-H) and 893.4 m/z (M-H) respectively. The mass to charge ratio of the fragments were searched against the database Metlin but no clear matches were found.

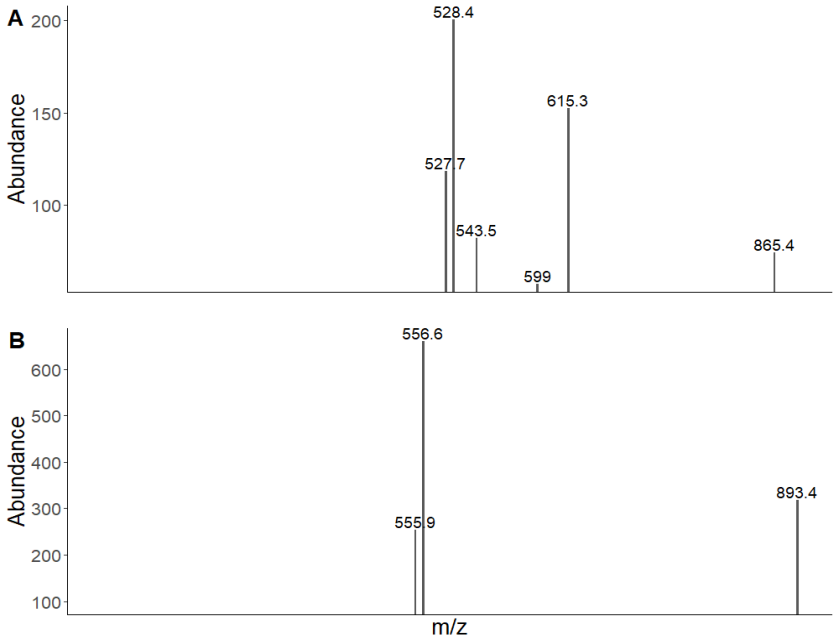

Figure 9. A: MS/MS spectrum of HPLC Peak 1. B: MS/MS spectrum of HPLC Peak 2. Both fragmentations were run with negative mode (M-H).

3.5 Microscopy and Species Composition

There is a visible variation in species composition between samples from the surface and the fluorescence layer, as well as between samples from Byfjorden and Havstensfjorden (Figure 10). A permANOVA resulted in a significant difference in species composition as a result of depth (pseudo-F = 9.06, p = 0.011), but not for location or depth by location interaction.

We found predominantly *Ceratium* spp., *Protoperidinium* spp. and *Pterosperma* spp. in the surface samples. *Ceratium* spp. were seven times more common in the surface samples than in the fluorescence layer samples, and centric diatoms were ten times more common in the fluorescence layer samples than in the surface samples. Otherwise, all observed species were exclusive to their collection depth. However, unidentifiable microorganisms formed the majority of the fluorescence layer samples.

There were no fluorescent microorganisms observed using the fluorescent microscope in either the untreated water sample or the samples fixed with Lugol's iodine solution.

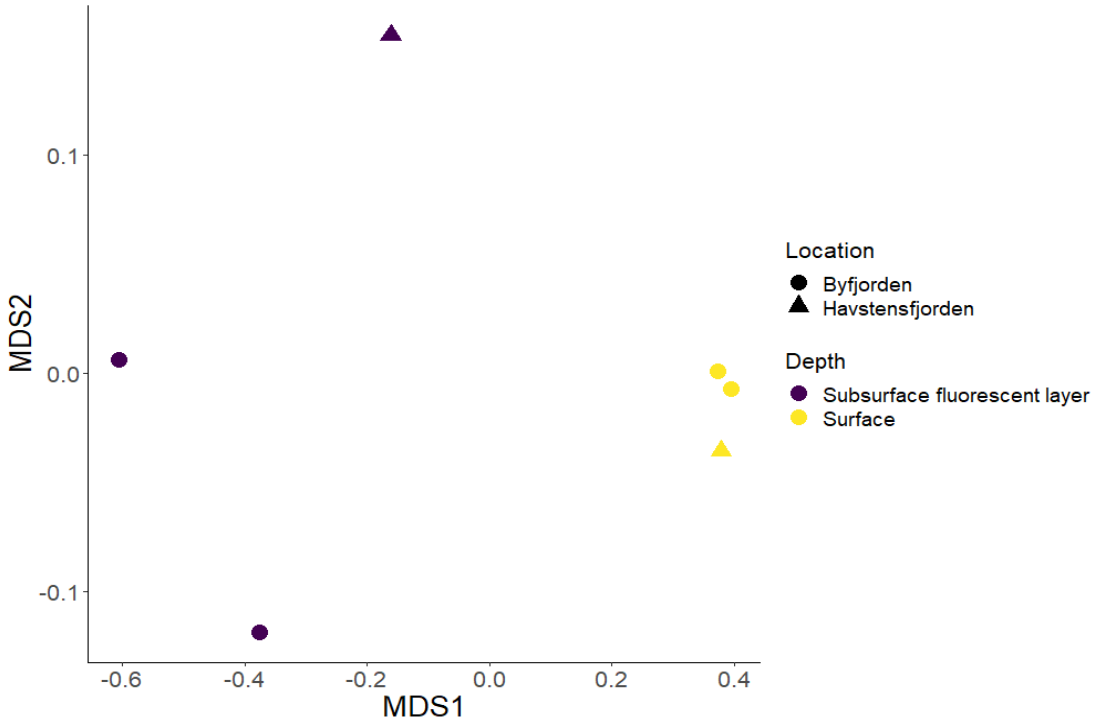

Figure 10. nMDS for species composition at the surface and subsurface fluorescent layer within Byfjorden and Havstensfjorden using Bray-Curtis dissimilarity. Stress value = 0.

4. Discussion

HPLC and Mass Spectrometry

Pigment analysis revealed some marked differences between the surface and subsurface fluorescence layer samples. The surface sample had a peak at 21.93 minutes which suggest that the sample contained chlorophyll *a* (Figure 6). When examining the absorption spectrum for this peak, it is evidently resembling that of the chlorophyll *a* standard (Figure 7). The absorption spectra of the surface sample and the chlorophyll *a* standard from our study are in accordance with scientific literature (e.g Roy *et al.,* 2011). This suggests that the method was carried out correctly and that the surface waters in Byfjorden contains pigments with chlorophyll *a*. This is consistent with the microscopic survey which showed that *Ceratium* sp., *Protoperidinium* sp. and *Pterosperma* sp. were the most common phytoplankton in the surface samples, which are known to contain chlorophyll *a* (Throndsen, 1997, Sheath and Wehr, 2003).

HPLC of the fluorescence layer samples resulted in a chromatogram with two distinct peaks at 15.98 and 16.91 minutes (Figure 6). The absorption spectra of these two peaks overlap each other, suggesting that the two peaks are homologs of the same pigment. Furthermore, these two absorption spectra show a great resemblance to that of bacteriochlorophyll *e* (Figure 8). Bacteriochlorophylls are found in anoxygenic phototrophic bacteria (Roy *et al.,* 2011). These bacteria perform photosynthesis but do not produce oxygen as a by-product. The anoxygenic phototrophic bacteria are found in four different major phylogenetic branches; the filamentous green and gliding bacteria, the green sulphur bacteria, the Heliobacteriaceae and the phototrophic purple bacteria (Imhoff, 2008). Among these groups, bacteriochlorophyll *e* is only found in the green sulphur bacteria. Bacteriochlorophyll *e* is a magnesium dihydroporphyrin with an isocyclic pentanone ring V and a propionic ester group at C17 (Figure 11). Bacteriochlorophyll *e* is not a single molecular form but a mixture of up to 15 homologs that mainly vary in the identity of alkyl groups at positions C8 and C12, in the chirality of the C31-center, and in the nature of the esterified alcohol at C17 (Borrego *et al.*, 1999). In the book Phytoplankton Pigments, edited by Roy *et al.* (2011), they state that LC-MS/MS have played an important role in the analysis of bacteriochlorophylls *c*, *d* and *e* as they exist as suites of compounds that are indistinguishable by UV/vis detection. The MS/MS carried out in this study examined the fragmentation of the mother ions of P1 and P2 (Figure 9). However, no matching compounds were found when searched against the Metlin data base. This could be due to errors in the method or lack of existing data for bacteriochlorophyll *e* homologs on Metlin. Nevertheless, this could point to the findings of novel

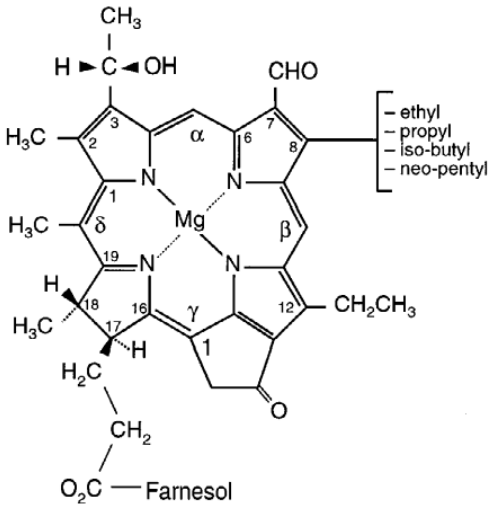

Figure 11. Chemical structure of bacteriochlorophyll e. From Borrego *et al.*, 1999.

structures. Further research and mass spectrometry should be done on the structure of this particular homolog of bacteriochlorophyll *e* to establish if this indeed is a new chemical structure.

Green sulphur bacteria are obligate anaerobic photoautotrophic bacteria that metabolize sulphur (Gregersen, Bryant and Frigaard, 2011). The photosynthetic apparatus of green sulphur bacteria, the chlorosomes, contains exceptionally large photosynthetic antennae (~1,500 bacteriochlorophyll molecules per reaction centre, Fowler *et al*., 1971). Consequently, these bacteria are capable of growth at significantly lower light intensities than other phototrophic organism (Overmann et al. 1992). Each chlorosome consists of a glycolipid monolayer envelope which encloses aggregates of bacteriochlorophylls *c*, *d* or *e*. Bacteriochlorophylls *c* and *d* are the major photosynthetic pigments in green species of green sulphur bacteria, while bacteriochlorophyll *e* is the major pigment in brown species (Imhoff, 1995). Green sulphur bacteria are most commonly found in freshwater lakes, lagoons, fjords, seas and marine sediments (Kushkevych *et al*., 2021) and have been found in habitats with similar conditions as Byfjorden. For example, Haas *et al.* (2018) observed a microbial mat in a flooded sinkhole in the Bahamas that consisted 74% of green sulphur bacteria. The sinkhole was meromictic with an upper freshwater layer separated from a lower saltwater column by a stable halocline. The mat they studied was located below the halocline at 30 m depth and in low-light conditions. They established that the microbial mat contained bacteriochlorophyll *e* by comparing the absorption spectrum and retention time of acetone-extracted photosynthetic pigments to previously published absorption spectra of bacteriochlorophyll *e*. These three published absorption spectra of bacteriochlorophyll *e* (Gloe *et al*., 1975; Borrego *et al*., 1999 and Haas *et al.*, 2018) match that of P1 and P2 in our study (Figure 7), with a maximum at 468 nm and a smaller peak at 651 nm. Furthermore, Haas *et al.* (2018) detected a variety of bacteriochlorophyll *e* homologs that all displayed the described absorption spectrum, but had different retention times ranging from 11.2 to 16.9 min.

The results from this study point towards green sulphur bacteria containing bacteriochlorophyll *e* being the cause of the subsurface fluorescence layer. It would be of interest to perform a genetic analysis of the water from the fluorescence layer to determine if green sulphur bacteria is present, and in that case, in what relative abundance. Suggested analysis is 16S rRNA gene sequencing and search against curated microbial databases.

CTD-Profiles and Fluorometric Analysis

The CTD profiles are in line with previous studies of Byfjorden (Figure 4, A, Stigebrandt and Liljebladh, 2010; Stigebrandt *et al.*, 2014) which states that the vertical mixing of the fjord is weak, leading to a long residence of deep-water and anoxia in the basin water below the halocline (Stigebrandt and Liljebladh, 2010). Green sulphur bacteria most commonly utilize sulphide, thiosulfate, biogenic and abiogenic sulphur globules, and H_2 as photosynthetic electron donors (Gregersen, Bryant and Frigaard,

2011) and are not dependent on oxygen for their metabolic pathways. A chemical analysis should be carried out to examine what compounds are present in the fluorescent layer.

Turbidity has a local maximum 2-3 m below the subsurface fluorescence layer (Figure 4, C). The peak in turbidity just below the subsurface fluorescence layer could be a result of matter accumulating at this depth due to a higher density of the deep-water. It could also be an accumulation of microorganisms residing at this depth, perhaps the same organisms that are causing the fluorescence peak. However, no fluorescent organisms were observed using the fluorescent microscope. The samples fixed with Lugol's iodine solution and the untreated samples were analysed approximately three weeks after collection. Potential fluorescent pigments of microorganisms could have degraded at this time. Future research could avoid this issue by analysing samples shortly after collection. Additionally, the peak in turbidity could be due to deposits from microorganisms residing around the 20 m depth. Green sulphur bacteria may produce sulphate from hydrogen sulphide or more oxidized sulphur compounds but can also produce elemental sulphur which is deposited extracellularly (Haas *et al.*, 2018). A chemical analysis should be carried out of the turbidity maximum to establish its contents and investigate any relationships between the turbidity and fluorescence maxima.

In conclusion, green sulphur bacteria with bacteriochlorophyll *e* is a probable cause of the mysterious subsurface fluorescence layer in Byfjorden. Genetic and chemical analyses should be carried out to prove their presence and to gain further understanding of the phenomenon.

5. References

5.1 Discussion

Borrego, C. M., Arellano, J. B., Abella, C.A., Gillbro, T. and Garcia-Gil, Jesús. (1999). The molar extinction coefficient of bacteriochlorophyll e and the pigment stoichiometry in Chlorobium phaeobacteroides. *Photosynthesis Research*, 60, 257–264. https://doi.org/10.1023/A:1006230820007

Fowler, C. F., Nugent, N. A. and Fuller, R. C. (1971) The isolation and characterization of a photochemically active complex from Chloropseudomonas ethylica. *Proc Natl Acad Sci USA*, 68, 2278–2282.

Gloe, A., Pfennig, N., Brockmann, H. and Trowitzsch, W. (1975). A new bacteriochlorophyll from brown-colored chlorobiaceae. *Archives of Microbiology*, 102, 103–109. https://doi.org/10.1007/BF00428353

Gregersen, L. H., Bryant, D. A and Frigaard, N. U. (2011). Mechanisms and evolution of oxidative sulfur metabolism in green sulfur bacteria. *Frontiers in Microbiology*. https://doi.org/10.3389/fmicb.2011.00116

Haas, S., de Beer, D., Klatt, J. M., Fink, A., Rench, R. M., Hamilton, T. L., Meyer, V., Kakuk, B. and Macalady, J. L. (2018) Low-Light Anoxygenic Photosynthesis and Fe-S-Biogeochemistry in a Microbial Mat. *Frontiers in Microbiology*. 9, 858. https://doi.org/10.3389/fmicb.2018.00858

Imhoff, J. F. (1995) Taxonomy and physiology of phototrophic purple bacteria and green sulfur bacteria. In: Blankenship RE, Madigan MT and Bauer CE (eds). *Anoxygenic Photosynthetic Bacteria*, pp. 1–15. Kluwer Academic, The Netherlands.

Imhoff, J.F. (2008). Systematics of Anoxygenic Phototrophic Bacteria. In: Hell, R., Dahl, C., Knaff, D., Leustek, T. (eds) *Sulfur Metabolism in Phototrophic Organisms*. Advances in Photosynthesis and Respiration, 27. Springer, Dordrecht. https://doi.org/10.1007/978-1-4020-6863-8_14

Kushkevych, I., Procházka, J., Gajdács, M., Rittmann, S. K. M. and Vítězová, M. (2021). Molecular physiology of anaerobic phototrophic purple and green sulfur bacteria. *International Journal of Molecular Sciences*, 22 (12), 6398.

Overmann, J., Cypionka, H. and Pfennig, N. (1992). An extremely low light adapted phototrophic sulfur bacterium from the Black Sea. *Limnol Oceanog*, 32, 150–155.

Roy, S. (Ed.). (2011). *Phytoplankton Pigments: Characterization, Chemotaxonomy, and Applications in Oceanography.* University Press, Cambridge.

Sheath, R. G. and Wehr, J. D. (2003). Introduction to Freshwater Algae. Wehr, J. D. and Sheath, R. G. (eds.). *Aquatic Ecology, Freshwater Algae of North America*. Academic Press, 1-9. ISBN 9780127415505. https://doi.org/10.1016/B978-012741550-5/50002-7

Stigebrandt, A., Liljebladh, B. (2010). Oxygenation of Large Volumes of Natural Waters by Geo-Engineering: with Particular Reference to a Pilot Experiment in Byfjorden. In: Badescu, V., Cathcart, R. (eds.) *Macro-engineering Seawater in Unique Environments*. Environmental Science and Engineering. Springer, Berlin, Heidelberg. https://doi.org/10.1007/978-3-642-14779-1_15

Stigebrandt, A., Liljebladh, B., de Brabandere, L., Forth, M., Granmo, Å., Hall, P., Hammar, J., Hansson, D., Kononets, M., Magnusson, M., Norén, F., Rahm, L., Treusch, A. H. and Viktorsson, L. (2015). An Experiment with Forced Oxygenation of the Deepwater of the Anoxic By Fjord, Western Sweden. *AMBIO*, 44, 42–54. https://doi.org/10.1007/s13280-014-0524-9

Throndsen, J. (1997). Chapter 5 - The Planktonic Marine Flagellates. Tomas, C.R (ed.). Identifying Marine Phytoplankton, *Academic Press*, 591-729, ISBN 9780126930184. https://doi.org/10.1016/B978-012693018-4/50007-0

5.2 Report

Andersen, C. M., & Nielsen, T. G. (2002). The effect of a sharp pycnocline on plankton dynamics in a freshwater influenced Norwegian fjord. Ophelia, 56(3), 135-160.

Baldry, K., Strutton, P. G., Hill, N. A., & Boyd, P. W. (2020). Subsurface chlorophyll-a maxima in the Southern Ocean. Frontiers in Marine Science, 7, 671.

Chen, R. F., Bissett, P., Coble, P., Conmy, R., Gardner, G. B., Moran, M. A., ... & Zepp, R. G. (2004). Chromophoric dissolved organic matter (CDOM) source characterization in the Louisiana Bight. Marine Chemistry, 89(1-4), 257-272.

Diaz, R. J., & Rosenberg, R. (2008). Spreading dead zones and consequences for marine ecosystems. science, 321(5891), 926-929.

Diaz, R. J., & Rosenberg, R. (1995). Marine benthic hypoxia: a review of its ecological effects and the behavioural responses of benthic macrofauna. Oceanography and marine biology. An annual review, 33, 245-03.

Franks, P. J. (1992). Sink or swim: Accumulation of biomass at fronts. Marine ecology progress series. Oldendorf, 82(1), 1-12.

Hartnett, H. (2018). Dissolved organic matter (DOM). In Encyclopedia of Earth Sciences Series (pp. 375-378). Springer Netherlands.

Helly, J. J., & Levin, L. A. (2004). Global distribution of naturally occurring marine hypoxia on continental margins. Deep Sea Research Part I: Oceanographic Research Papers, 51(9), 1159-1168.

Imhoff, J. F. (1992). Taxonomy, phylogeny, and general ecology of anoxygenic phototrophic bacteria. In Photosynthetic prokaryotes (pp. 53-92). Springer, Boston, MA.

Klausmeier, C. A., & Litchman, E. (2001). Algal games: The vertical distribution of phytoplankton in poorly mixed water columns. Limnology and Oceanography, 46(8), 1998-2007.

Kononen, K., Huttunen, M., Hällfors, S., Gentien, P., Lunven, M., Huttula, T., ... & Stips, A. (2003). Development of a deep chlorophyll maximum of Heterocapsa triquetra Ehrenb. at the entrance to the Gulf of Finland. Limnology and Oceanography, 48(2), 594-607.

Koskinen, K., Hultman, J., Paulin, L., Auvinen, P., & Kankaanpää, H. (2011). Spatially differing bacterial communities in water columns of the northern Baltic Sea. FEMS microbiology ecology, 75(1), 99-110.

Legović, T., Viličić, D., Petricioli, D., & Žutić, V. (1991). Subsurface Gonyaulax polyedra bloom in a stratified estuary. Marine chemistry, 32(2-4), 361-374.

Lips, U., Lips, I., Liblik, T., & Kuvaldina, N. (2010). Processes responsible for the formation and maintenance of sub-surface chlorophyll maxima in the Gulf of Finland. Estuarine, Coastal and Shelf Science, 88(3), 339-349.

Nielsen, T. G., Kiørboe, T., & Bjørnsen, P. K. (1990). Effects of a Chrysochromulina polylepis subsurface bloom on the planktonic community. Marine Ecology Progress Series, 21-35.

Padmakumar, K. B., Thomas, L. C., Salini, T. C., Vijayan, A., & Sudhakar, M. (2018). Subsurface bloom of dinoflagellate Gonyaulax polygramma Stein in the shelf waters off Mangalore-South Eastern Arabian Sea.

Perry, M. J., Sackmann, B. S., Eriksen, C. C., & Lee, C. M. (2008). Seaglider observations of blooms and subsurface chlorophyll maxima off the Washington coast. Limnology and Oceanography, 53(5part2), 2169-2179.

Rabalais, N. N., Diaz, R. J., Levin, L. A., Turner, R. E., Gilbert, D., & Zhang, J. (2010). Dynamics and distribution of natural and human-caused hypoxia. Biogeosciences, 7(2), 585-619.

Röttgers, R., & Koch, B. P. (2012). Spectroscopic detection of a ubiquitous dissolved pigment degradation product in subsurface waters of the global ocean. Biogeosciences, 9(7), 2585-2596.

Saini, D. K., Pabbi, S., & Shukla, P. (2018). Cyanobacterial pigments: Perspectives and biotechnological approaches. Food and chemical toxicology, 120, 616-624.

Stedmon, C. A., & Nelson, N. B. (2015). The optical properties of DOM in the ocean. In Biogeochemistry of marine dissolved organic matter (pp. 481-508). Academic Press.

Stigebrandt, A., & Liljebladh, B. (2010). Oxygenation of large volumes of natural waters by geo-engineering: with particular reference to a pilot experiment in Byfjorden. In Macro-engineering Seawater in Unique Environments (pp. 303-315). Springer, Berlin, Heidelberg.

Yurkov, V. V., & Beatty, J. T. (1998). Aerobic anoxygenic phototrophic bacteria. Microbiology and Molecular Biology Reviews, 62(3), 695-724.

6. Appendix

Table 1. Coordinates for sampling Stations

Station	Latitude	Longitude
Station-1	58.342233	11.903433
Station-2	58.33874	11.892271
Station-3	58.33675	11.883345
Station-4	58.33355	11.874717
Station-5	58.32865	11.85639
Station-6	58.32491	11.835283
Station-7	58.317967	11.805867
Station-8	58.314268	11.77537
Station-1 2022/09/18	58.33777	11.89805

Table 2. Volume of water pumped through vacuum pump to obtain pigment residue.

Sample no.	**Volume of Water**
Stn.-1, 5 meters	400 mL
Stn.-3, 7 meters	400 mL
Stn.-5, 5 meters	400 mL
Stn.-3, 21 meters	200 mL
Stn.-4, 20 meters	150 mL
Stn.-1,~20 meters 2022/09/18	200 mL

Table 3. Number of species at each station.

Species Name	Station-1 5 meters	Station-5 5 meters	Station-7 7 meters	Station-3 21 meters	Station-4 20 meters	Station-7 20 meters
Amoeba	0	0	0	0	17	0
Centric Diatoms	0	1	0	0	10	0
Ceratium Horridium	2	0	0	0	0	6
Ceratium Fusus	25	24	58	0	0	
Ceratium lineatum	272	85	259	0	5	85
Copepod	2	1	0	0	0	5
Copepod Eggs	0	0	0	0	0	11
Cylindrotheca closertium	48	0	12	0	0	0
Unidentified species	0	0	0	7107	0	0
Dictyocha sp.	3	0	4	0	0	0
Dinoflagellate cyst	0	4	0	0	0	0
Ditylum sp.	0	3	5	0	0	0
Gyordium/ Gynodium	177	146	99	0	0	0
Katodinium sp.	0	0	0		6	
Larvae	0	0		3429	4970	99
Loricate ciliate	20	3	2	0	0	0
Nauplii	0	1	0	0	0	0

Noctilucans sp.	0	1	3	0	0	0
Prorocentrum micans	42	11	26	0	0	0
Procentrum sp.	0	0	0	158	1064	55
Protoperidium sp.	308	102	77	0	0	0
Pseudonitschia sp.	1	1	0	0	0	0
Pterosperma sp.	206	150	28	0	0	0
Rhizosole sp.	5	0	1	0	0	0
Skeletonema sp.	12	2	4	0	0	0

Calculation 1. Calculation of outflow from HPLC system

We estimated the width of the outflow tube to be one fourth of an inch, with a total length of 75 cm. The flow rate of the HPLC system was set to 0.8 ml per second. From this we calculated the time frame in which the sample cycled through the system after the peak was detected. This time was approximately 10 seconds.